COMPARATIVE ANALYSIS OF HOMOLOGOUS BUILDINGS USING RANGE IMAGING

Li Ding[1], *Ahmed Elliethy*[1], *Eitan Freedenberg*[3], *S. Alana Wolf-Johnson*[3], *Joshua Romphf*[4], *Peter Christensen*[2], *Gaurav Sharma*[1]

[1]Dept. of Electrical and Computer Engineering, [2]Dept. of Art and Art History,
[3]Graduate Program in Visual and Cultural Studies, [4]River Campus Libraries,
University of Rochester, Rochester, NY

ABSTRACT

This paper reports on a novel application of computer vision and image processing technologies to an interdisciplinary project in architectural history that seeks to help identify and visualize differences between homologous buildings constructed to a common template design. By identifying the mutations in homologous buildings, we assist humanists in giving voice to the contributions of the myriad additional "authors" for these buildings beyond their primary designers. We develop a framework for comparing 3D point cloud representations of homologous buildings captured using lidar: focusing on identifying similarities and differences, both among 3D scans of different buildings and between the 3D scans and the design specifications of architectural drawings. The framework addresses global and local alignment for highlighting gross differences as well as differences in individual structural elements and provides methods for readily highlighting the differences via suitable visualizations. The framework is demonstrated on pairs of homologous buildings selected from the Canadian and Ottoman rail networks. Results demonstrate the utility of the framework confirming differences already apparent to the humanist researchers and also revealing new differences that were not previously observed.

Index Terms— architectural biometrics, building difference visualization, point cloud comparison, range imaging, visual big data analytics

1. INTRODUCTION

Recent advances in the sensors used for lidar 3D scanners have substantially reduced their cost spurring an increase in the number of applications for which they are deployed. In addition to science and engineering, lidar is also finding novel applications in the humanities and social sciences. We report on one such application in an interdisciplinary collaborative project, Architectural Biometrics [1], that uses lidar scanning along with computer vision and image processing technologies to address humanistic concerns in architectural history. Specifically, the Architectural Biometrics project aims at identifying distinguishing characteristics of buildings built to a common design template with a view to identifying their unique "biometric" identities. The humanistic goal of such comparison is to recognize the contributions of the engineers, tradespersons, and laborers who contributed to the on-site construction of each building, individuals who are often disenfranchised by attribution of the building to the architects and designers alone. In analogy with Biology where genomic subsequences (and their derivatives such as proteins) obtained from a common ancestor are referred to as homologs, we refer to the buildings designed to a common design template as homologs and to the differences among them as mutations. Here, we focus specifically on an **algorithmic framework for comparison of homologous buildings to highlight similarities and differences both among the buildings and with respect to plan documents and on methods for visualizing the similarities and differences**. Other ongoing work within the project, conflates the analyses we present here with additional data sources such as census logs to determine how the unique identifying characteristics that we determine correlate with the cultural backgrounds of the individuals that contributed to the mutational changes.

We demonstrate the applicability and utility of our algorithmic framework using datasets consisting of lidar scan data and design drawings for buildings from the Canadian and Turkish-Ottoman railways. Both sets of buildings represent railway stations designed to templated plans and include at least a pair of homologous buildings for each design template. In prior work based purely on conventional images and visual comparison, several fascinating differences between some of these buildings have already been noted [2]. Results obtained with the framework we present here, validate these already known differences and highlight several new ones.

While the Architectural Biometrics project is unique, related work exists in several contexts. Change detection in laser-scanned data has previously been addressed in data acquired from the same industrial site [3] or buildings [4] at two different points in time. The temporal changes are, however, different from the fundamental structural changes seen in homologous buildings in that large parts remain unaltered between scans at two points in time. Also these situations do not require or address the relationship of the building plans to the lidar data, a problem that poses new challenges due to the different modalities and representations of the data. There are also other recent works that use visual/lidar datasets for architectural analyses and comparisons, albeit for unrelated problems. In particular, [5] seeks to identify frequent and discriminative characteristics representative of a city's architecture from photographic data available on Google Street Maps. Lidar data has also been extensively utilized in mapping archaeological sites [6, 7].

The paper is organized as follows. Section 2 describes our input datasets and the questions we seek to answer and highlights the challenges. A sketch of our proposed framework is outlined in Section 3. Experimental results are presented in Section 4 highlighting how our automated analyses augments the preliminary visual observations of the humanities scholars. Concluding remarks and discussion summarize the main findings in Section 5.

2. DATASETS, QUESTIONS, AND CHALLENGES

Before presenting our framework, we first:

- describe the datasets we work with thereby also establishing the notation for subsequent development,
- list the questions of interest for our analyses, which motivate the framework we develop, and
- highlight several of the technical challenges encountered in addressing these questions.

This project was supported in part by a University Research Award from the University of Rochester.

The input data are comprised of point clouds of the buildings of interest obtained from lidar scanning and architectural design drawings. The point cloud data for the i^{th} building is given by

$$L_i = \{(B_l^i, V_l^i)\}_{l=1}^{N_i}, \quad i = 1, 2, \ldots K \tag{1}$$

where $B_l^i = \left(x_l^i, y_l^i, z_l^i\right)^T \in \mathbb{R}_+^3$ are the 3D coordinates of the l^{th} point in space and $V_l^i = (R_l^i, G_l^i, B_l^i)^T \in \mathbb{R}_+^3$ is the RGB color value for the point, N_i is the number of points in the point cloud and K is the number of buildings, $\mathbb{R}_+$ denotes the set of nonnegative real numbers, and the superscript ^{T} denotes the transpose operation. The architectural drawings for the building consist of a plan-view and four elevation views. We represent these as binary images. Specifically, each view is represented as a set of 2D pixel locations corresponding to the outer contour for the given view: $D_v = \{b_m^v\}_{m=1}^{M_v}$, where $b_m^v = (\xi^v, \eta^v)$ represents a pixel location on the outer contour and $v = 1, 2, \ldots 5$ represents the index for the view.

Given the data, motivated by the analyses that the architectural historians would like to conduct, we are interested in answering three questions: **(1) Are there fundamental *structural* differences between the homologs? (2) Do the constructed buildings differ from the template provided in their specifications of architectural drawings?, and (3) Are there similarities among the deviations in individual buildings that share a common template specification?** Rather just than yes/no answers to these questions, we are interested in both visualizing the similarities and differences in a meaningful manner and in quantifying these. To do so, however, is not entirely trivial because of several challenges. Firstly, before any comparisons can be made between different point clouds they need to be registered to align corresponding structural components, such registration also needs to comprehend and handle the differences between the different buildings. A similar challenge is encountered in the comparison of the point clouds against the plan drawings, where additionally the fundamentally different modalities of the data 3D points vs binary images representing the plan and elevation views also needs to be meaningfully tackled. Last, but not least, any methods we develop must work despite the different numbers of points in different datasets and the inevitable missing data and outliers. Particularly in the lidar 3D scans where the accessible vantage points for placing the scans often prevent imaging of surface locations in certain parts of the building structure, in particular portions of the roof. In the following section, we present an algorithmic framework for addressing these questions and overcoming the challenges.

3. BUILDING HOMOLOG COMPARISON FRAMEWORK

Our proposed framework for homologous buildings comparison consists of three steps: global alignment, Hough clustering and difference quantification and visualization. The block diagram of Fig. 1 shows the main elements of our methodology. The inputs are scanned buildings, both of which are point clouds generated by 3D laser scanner, as well as the design specification plan and elevation drawings. After global alignment, we use 3D Hough clustering method to detect planar substructures of the buildings. Finally, the difference is quantified based on a distance-based computation.

Point cloud alignment: Since the initial location and pose of captured point clouds are different, it is necessary to first determine the correspondence between two sets of points and map them to a common reference. Adopting a rigid transformation which is defined by a unitary rotation matrix $\mathbf{R}_{3\times3}$, a translation vector $\mathbf{t}_{3\times1}$, and a positive scaling parameter s, a procedure of global alignment can be

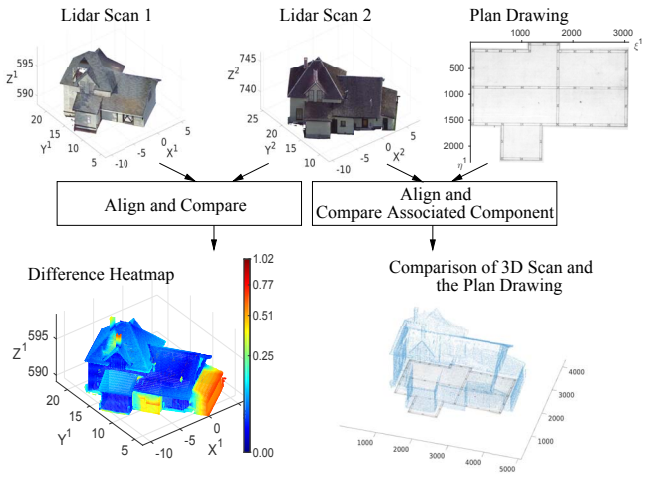

Fig. 1: Overview of the proposed methodology for comparison of homologous buildings. Lidar Scan 1 and Scan 2 represent two Canadian railway stations Turtleford and Meeting Creek, respectively.

defined by minimizing the objective function

$$Q_0 = \sum\nolimits_k \| B_k^i - s\mathbf{R}_{3\times3} B_k^j - \mathbf{t}_{3\times1} \|^2, \tag{2}$$

where B_k^i and B_k^j are corresponding points for the two scans L_i and L_j, respectively.

In actual practice, the scans have different number of data points and, possibly, missing data and outliers. To accommodate these possibilities, latent variables χ_{mn} are introduced for assessing putative correspondences between points B_n^j in L_j and B_m^i in L_i, where $\chi_{mn} = 1$ if the points correspond and 0 otherwise. The objective function of (2) is then modified to [8]

$$\begin{aligned} Q = &\sum\nolimits_{m,n=1}^{N_i,N_j} p_{mn} \| B_m^i - s\mathbf{R}_{3\times3} B_n^j - \mathbf{t}_{3\times1} \|^2 \\ &- \lambda_1 \sum\nolimits_{m,n=1}^{N_i,N_j} -p_{mn} \log p_{mn} - \lambda_2 \sum\nolimits_{m,n=1}^{N_i,N_j} p_{mn}, \end{aligned} \tag{3}$$

where p_{mn} is the probability that χ_{mn} is 1, and the two additional terms provide regularization. The second term in (3) is the sum of the entropy of all p_{mn}. This term is maximized when $p_{mn} = 1/N_i N_j$, which means that all points are forced to the same error and thus move smoothly. The third term serves to maximize the probability of correspondence. Several methods have been proposed for such problems [8]. In particular, we employ the CPD algorithm [9] for global alignment that is able to simultaneously determine the transformation and the correspondence probabilities p_{mn}.

Point cloud and design drawing alignment: The point clouds and the design specification drawings represent fundamentally different data representations. To align them, we proceed sequentially, first aligning the vertical projection of the point cloud (known from the scanning geometry) to the plan view (assumed to correspond to $v = 1$), and then aligning the projections of the point cloud along the appropriate elevation directions (known from the alignment to the plan) to the corresponding elevation views.

The alignment of the i^{th} point cloud to the v^{th} view is accomplished as follows. First we compute $\mathbf{P}_v B_l^i$, where $\mathbf{P}_v$is the projection matrix along the direction corresponding to the v^{th} view, and identify the set of N_c^i points, with indices $l_{j_1}, l_{j_2}, \ldots, l_{j_{N_c^i}}$, that correspond to the outer contour. Then we determine the rotation matrix

$\mathbf{R}_{2\times2}$. the translation vector $\mathbf{t}_{2\times1}$, and the scaling parameter s that minimize the sum of squared minimum distance between the transformed location $\left(s\mathbf{R}_{2\times2}\mathbf{P}_v B^i_{l_j} + \mathbf{t}_{2\times1}\right)$ and the nearest point from $\{b^v_m\}^{M_v}_{m=1}$ as

$$(\mathbf{R}^*_{2\times2}, \mathbf{t}^*_{2\times1}, s^*) = \underset{\mathbf{R}_{2\times2},\mathbf{t}_{2\times1},s}{\arg\min} \sum_{r=1}^{N^i_c} \min_m \|s\mathbf{R}_{2\times2}\mathbf{P}_v B^i_{l_{jr}} + \mathbf{t}_{2\times1} - b^v_m\|^2. \quad (4)$$

The minimum distance is efficiently computed by using the distance transform [10] and the minimization in (4) can be recognized as chamfer minimization [11].

Hough clustering: Inspired by the observation that most architectural structures in the building are characterized by planes, e.g., walls, roofs, ceilings and so forth, planar parts are preferable elements for comparing local differences. We therefore use 3D Hough clustering to identify the dominant planar substructures in the point clouds. Hough transform [12, 13] is a robust method for analysis of parametrized elements in images, e.g., straight lines and circles, but can be readily extended to the 3D scenario in which the input data is a point cloud in ^{3}. In general, plane is modeled by a set of Hough space parameter (ϕ, θ, ρ).

$$\rho = \left(x^i_l \cos\phi + y^i_l \sin\phi\right)\cos\theta + z^i_l \sin\theta. \quad (5)$$

One challenging problem is that the parameters of adjacent planes may be close in Hough space posing challenging for resolution as independent planes. Hence, in the process of searching local maximum value that indicates a dominant planar structure, we are not able to properly detect the plane that has few points. To solve it, we set up two thresholds T_1 and T_2 $(T_1 > T_2)$ to constrain the minimum number of points in detected planes, and perform the Hough clustering in two steps. The first step aims to detect large dominant planes within building and extract them from the point cloud by specifying the minimum number of points T_1 within the plane. Inlier points affiliated with these planes are then removed and 3D Hough clustering is applied to the remaining points with the smaller threshold T_2, allowing detection of smaller planar substructures.

Difference quantification: In this stage, we propose a distance-based measurement to infer and quantify the differences between homologous buildings. The normalized Euclidean distance which also balances the scale factors of different variables is used to measure distances. Because the CPD algorithm is able to indicate the correspondence between two point sets, we calculate distance $d^{L_j}_{L_i}$ from the target point cloud L_j to the reference one L_i based on the corresponding points

$$d^{L_j}_{L_i} = \frac{1}{N_j}\sum\nolimits_{l=1}^{N_j} d_E\left(B^i_{l_c}, B^j_l\right), \quad (6)$$

where $B^i_{l_c}$ is the point in the reference point cloud L_i that is the estimated maximum aposteriori probability (MAP) correspondence for the point B^j_l in the target point cloud L_j, and $d_E\left(B^i_{l_c}, B^j_l\right)$ is the normalized Euclidean distance between two points $B^i_{l_c} = \left(x^i_{l_c}, y^i_{l_c}, z^i_{l_c}\right)$ and $B^j_l = \left(x^j_l, y^j_l, z^j_l\right)$

$$d_E\left(B^i_{l_c}, B^j_l\right) = \sqrt{\frac{\left(x^i_{l_c} - x^j_l\right)^2}{\sigma_x^2} + \frac{\left(y^i_{l_c} - y^j_l\right)^2}{\sigma_y^2} + \frac{\left(z^i_{l_c} - z^j_l\right)^2}{\sigma_z^2}}, \quad (7)$$

where σ_x^2, σ_y^2 and σ_z^2 are the variances of X-, Y- and Z-coordinate in the reference point cloud L_i, respectively. Notice that the distance in (6) is asymmetric. To symmetrize, the distance between two point clouds L_i and L_j is defined by

$$d_{PC}\left(L_i, L_j\right) = \frac{1}{2}\left(d^{L_j}_{L_i} + d^{L_i}_{L_j}\right). \quad (8)$$

The minimum chamfer distance in (4) provides a quantification of the difference between the point cloud and design specifications. Also, these distances are readily localized to compute the deviation for each point in the target point cloud, which can then be visualized. Similarly differences in local features are also computable after alignment of corresponding planar substructures identified using Hough clustering with associations.

4. EXPERIMENTS AND RESULTS

Our datasets of scanned buildings contain 13 railway stations from Canada and Turkey, each built as part of a design specification set. The lidar datasets are gathered by the FARO Focus 3D X330 laser scanner [14], which has a distance measurement accuracy of $\pm$2 mm. The point cloud data for each building comprises 10 to 22 million points, ranging from 1.5 to 2.5 gigabytes in a compressed format. Although the datasets provide many comparative results, here we present only a small subset for illustration.

Global comparison: We choose 9 railway stations for analysis based on the levels of completeness and accuracy of point clouds. Figure 2 is an example showing the global comparison of two point clouds, which represent the homologous buildings, Ayrancı and Demiryurt, from Turkey. Initially, we choose Ayrancı as the target point cloud and show the results of comparison in the first row of Fig. 2, then exchange the roles of the point clouds and plot the results of comparing Demiryurt in the second row of Fig. 2. The examples of global alignments are shown in Figs. 2b and 2e. The reference point cloud is shown as magenta points, while the target point cloud is represented by green points. The result shows that two point clouds are successfully overlaid in alignment. After applying global alignment between two sets of points, the point-point distance is calculated using (7). In Figs. 2c and 2f, heat maps are rendered to visualize the distance from the target point cloud to the reference point cloud. The regions that are detected to have significant difference are highlighted with red and yellow, while the points in deep blue are identified as similarities between the two point clouds. It is important to point out that the heat map in Fig. 2c has a red region on the roof, which is due to the lack of data in that area for the reference point cloud and thus corresponds to the difference. Another example of comparing two Canadian buildings, Meeting Creek and Turtleford, can be seen in the examples used in Fig. 1. We can see that, in the heat map, the different regions is automatically detected, e.g., chimney and two additional sheds in Meeting Creek. **While the differences in the sheds were already noted by the humanities scholars studying these buildings, the chimney differences were first noted upon seeing out post alignment visualization.** Further examination of the data revealed that Turtleford, while closely related to Meeting Creek, was not strictly a homolog as per our definition. This also highlighted the value of the automated analysis proposed here in identifying buildings of the same "genus" but not necessarily identical species.

We take another group of near homologous buildings, which consists of Waldheim, Meeting Creek and Turtleford, as an example to show the comparison between the point clouds and their design drawings. Figure 3 shows the end elevation and the rear elevation drawings (plan drawing is depicted in Fig. 1). **Figure 4 reveals not**

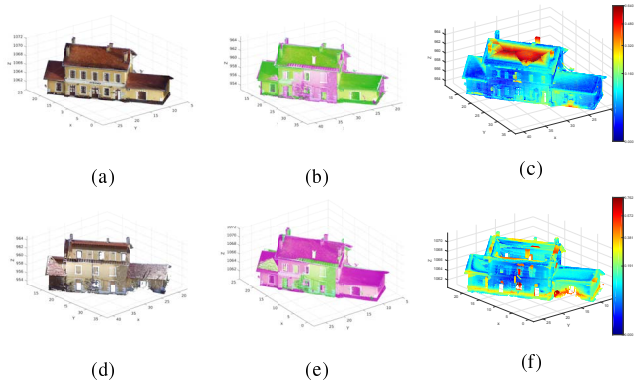

Fig. 2: Sample results for a pair of homologous buildings from the Baghdad Railway in Turkey [2]: (a) and (d) are the individual point clouds from laser scans of Ayrancı and Demiryurt, respectively; (b) and (e) show the result after global alignment; (c) and (f) show the differences between the aligned clouds as heat maps.

only the large scale divergences, e.g., the additional shed, but also the small differences, e.g., the angle of the roofs, from the design drawings. These differences were not previously noted by the humanities scholars. We compute the chamfer distances between the point cloud and the associated component of the drawing using (4). The end elevation and rear elevation drawings both have front view and back view. We take the average value of chamfer distances for these two views and list the results in Table 1. We can see that **Turtleford best matches the design drawing and that Waldheim and Meeting Creek are quite close to each other, despite having more mutations with respect to the drawings. Importantly, our comparisons also revealed an error in the specification drawings where a chimney was missing in one of the elevation views.**

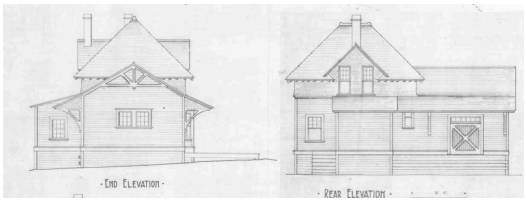

Fig. 3: The end and rear elevation drawings for three near homologous buildings from the Canadian National Railway [15].

Fig. 4: Sample result of comparison of 3D scan of Waldheim against elevation drawings. The magenta points are the projection of the point cloud along the the direction corresponding to the given drawing, and the blue line represents the outer contour for the view of elevation drawing.

Local comparison: From the result of global alignment of point clouds, we can readily find the small displacement of alignment, which results in inaccuracy of the local comparison. We apply aforementioned clustering method to detect vertical planar parts in the processed point clouds. The planar models extracted from Meeting Creek and Turtleford are shown in Figs. 5a and 5d, respectively. The corresponding planar models are highlighted as the same color, while the red planes in Fig. 5a are identified as outlier planes. We extract the cyan planes from the point clouds, which are shown in Figs. 5b and 5e, to illustrate the local comparison. Figures 5c and 5f show the heat maps of the selected walls. **The difference can be observed in the window and in the bottom of the wall. A comparison between the heat map in Fig. 1 and Fig. 5c shows medium scale differences, which are not highlighted in global comparison, but detected by the Hough clustering.**

	Building Name		
	Waldheim	Meeting Creek	Turtleford
Ground	83.23	68.80	11.79
End Elevation	19.17	20.06	38.40
Rear Elevation	35.91	42.26	26.83

Table 1: Comparison of point cloud scan data against the design specification plan and elevation drawings for three buildings from the Canadian Northern Railway.

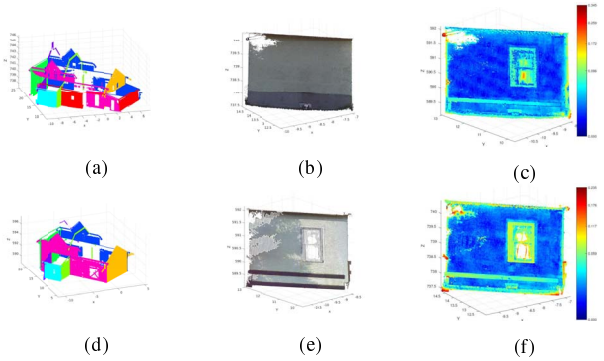

Fig. 5: Results of 3D Hough clustering of the point cloud datasets and local comparison. (a) and (d) show the Hough clustering for Meeting Creek and Turtleford as different colors that are readily seen to be the planar components of the structures. (b) and (e) show corresponding region of selected planar components for comparison and (c) and (f) show the differences.

5. CONCLUSION

The framework we present in this paper provides an effective methodology for the comparison of homologous buildings built to a common specification. Using 3D point cloud dataset obtained via lidar scanning and architectural specification drawings and developing appropriate methods for aligning and comparing these datasets and drawings, our framework allows differences between the buildings to be visualized and quantified. Results obtained from deploying the framework on two datasets corresponding to the Canadian and Ottoman railroads demonstrate that the framework reveals not only differences that are immediately apparent to architectural historians upon visual inspection but also other subtle differences both at global and local scales. The framework provides a valuable tool for humanistic studies. Beyond the immediate application of visualizing and quantifying differences further analysis using the framework also shows its utility in automatic classification into homologous categories and in identifying the correspondence and deviations from design specifications.

6. REFERENCES

[1] "Architectural biometrics project website." [Online]. Available: http://www.architecturalbiometrics.com

[2] P. Christensen, "Architecture, Expertise, and the German Construction of the Ottoman Railway Network, 1868-1919," Ph.D. dissertation, Harvard University, 2014.

[3] J. Huang and S. You, "Change detection in laser-scanned data of industrial sites," in *IEEE Workshop on Appl. of Comp. Vision.*, Jan 2015, pp. 733–740.

[4] Z. Kang, L. Zhang, H. Yue, and R. Lindenbergh, "Range image techniques for fast detection and quantification of changes in repeatedly scanned buildings," *Photogrammetric Engineering & Remote Sensing*, vol. 79, no. 8, pp. 695–707, 2013.

[5] C. Doersch, S. Singh, A. Gupta, J. Sivic, and A. Efros, "What makes Paris look like Paris?" *ACM Trans. on Graphics*, vol. 31, no. 4, 2012.

[6] R. Hesse, "LiDAR-derived local relief models a new tool for archaeological prospection," *Archaeological Prospection*, vol. 17, no. 2, pp. 67–72, 2010. [Online]. Available: http://dx.doi.org/10.1002/arp.374

[7] A. F. Chase, D. Z. Chase, C. T. Fisher, S. J. Leisz, and J. F. Weishampel, "Geospatial revolution and remote sensing LiDAR in Mesoamerican archaeology," *Proc. Nat. Acad. Sci.*, vol. 109, no. 32, pp. 12 916–12 921, 2012.

[8] G. K. Tam, Z.-Q. Cheng, Y.-K. Lai, F. C. Langbein, Y. Liu, D. Marshall, R. R. Martin, X.-F. Sun, and P. L. Rosin, "Registration of 3d point clouds and meshes: a survey from rigid to nonrigid," *IEEE Trans. Visual and Computer Graphics*, vol. 19, no. 7, pp. 1199–1217, 2013.

[9] A. Myronenko and X. Song, "Point set registration: Coherent point drift," *IEEE Trans. Pattern Anal. Mach. Intel.*, vol. 32, no. 12, pp. 2262–2275, Dec 2010.

[10] G. Borgefors, "Distance transformations in digital images," *Comp. Vis., Graphics and Image Proc.*, vol. 34, no. 3, pp. 344–371, 1986.

[11] H. G. Barrow, J. M. Tenenbaum, R. C. Bolles, and H. C. Wolf, "Parametric correspondence and chamfer matching: Two new techniques for image matching," in *Proc. Int. Joint Conf. Artificial Intell.*, 1977, pp. 659–663.

[12] R. O. Duda and P. E. Hart, "Use of the Hough transformation to detect lines and curves in pictures," *Commun. ACM*, vol. 15, no. 1, pp. 11–15, 1972.

[13] D. Borrmann, J. Elseberg, K. Lingemann, and A. Nüchter, "The 3D Hough transform for plane detection in point clouds: A review and a new accumulator design," *3D Research*, vol. 2, no. 2, pp. 1–13, 2011.

[14] *Focus3D X 330 Tech Sheet*, Faro Technologies, Oct. 2013. [Online]. Available: http://www.faro.com/products/3d-surveying/laser-scanner-faro-focus-3d/downloads?category=Technical%20Sheets#Download

[15] "Canadian northern railway company - drawings of standard third class station building (n0120031)," Library and Archives Canada, 395 Wellington Street, Ottawa, ON K1A 0N4, Aug 1907, accessed June 2015.